ORNL/TM-2022/2564

Review of Thermal Contact Resistance of Flexible Graphite Materials for Thermal Interfaces in High Heat Flux Applications

Adrian S. Sabau

September 2022

OAK RIDGE National Laboratory

ORNL IS MANAGED BY UT-BATTELLE LLC FOR THE US DEPARTMENT OF ENERGY

ORNL/TM-2022/2564

Computational Sciences and Engineering Division

REVIEW OF THERMAL CONTACT RESISTANCE OF FLEXIBLE GRAPHITE MATERIALS FOR THERMAL INTERFACES IN HIGH HEAT FLUX APPLICATIONS

Adrian S. Sabau

August 2022

Prepared by
OAK RIDGE NATIONAL LABORATORY
Oak Ridge, TN 37831
managed by
UT-BATTELLE LLC
for the
US DEPARTMENT OF ENERGY
under contract DE-AC05-00OR22725

CONTENTS

TABLE OF CONTENTS

LIST OF FIGURES

LIST OF TABLES

ACKNOWLEDGMENTS

This work was sponsored by the Office of Fusion Energy Sciences under contract DE-AC05-00OR22725 with UT-Battelle, LLC.

ABSTRACT

In this report, the data on thermal contact conductance and/or thermal contact resistance (TCR) at material interfaces, which employs flexible graphite (FG) materials as thermal interface materials (TIM), is reviewed. FG materials are often used as TIM due to their conforming nature. While the overall TCR can be estimated straightforward from measured data, the interface TCR is much more difficult to obtain. This report also discusses the interfacial thermal contact conductance between FG-tungsten and FG-Glidcop-Al15, which are envisioned for high-heat flux applications.

1 THERMOPHYSICAL AND THERMOMECHANICAL PROPERTIES OF FLEXIBLE GRAPHITE

Commercial flexible graphite (FG) materials are often referred by the Grafoil tradename [1]. An extensive review on FG thermophysical properties is given in [1, 2]. However, it is only recently that the mechanical properties were fully characterized [3]. The following elastic and inelastic mechanical properties were reported in [3]:

- Young's modulus, E = 190 MPa
- Poisson's ratio, $\nu = 0.3$
- Yield stress, $\sigma_Y = 1.9$ MPa
- Hill's parameters, F = G = H = 0.5, L = M = N = 1.5
- Isotropic hardening modulus, Q= 0.7 MPa
- Non-linear isotropic hardening coefficient, b = 13

For flexible graphite, the following average hardness values of 16.0, 10.9, 7.3, and 5.8 MPa were measured in [3] based on nanoindentation experiments for loads of 0.1, 0.25, 0.5, and 1 mN, respectively.

2 FACTORS AFFECTING JOINT AND INTERFACE THERMAL CONTACT CONDUCTANCE

The general configuration considered is that of FG thermal interface materials (TIM) sandwiched between hard metallic surfaces (Figure 1). Depending on the contact nature, two configurations can be considered: (a) contacting surfaces and (b) non-contacting surfaces. Thermal contact resistance, TCR_J, or its reciprocal, thermal contact conduction, TCC_J, for the overall joint is estimated directly using the measured data for temperature (i.e., $T_{i,1,1}$, and $T_{i,2,1}$ as shown in Figure 1) and heat flux across the TIM joint, $q''_{J,TIM}$.

$$\boldsymbol{TCR_{J,TIM} = \frac{T_{i,1,1} - T_{i,2,1}}{q''_{J,TIM}}}, \text{ and } \boldsymbol{TCC_{J,TIM} = \frac{1}{TCR_{J,TIM}}} \quad \textbf{(1)}$$

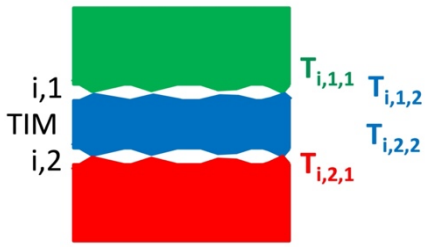

Figure 1. Soft TIM between hard materials.

By considering the elastic deformation of the TIM and the temperature variation of the thermal conductivity of the TIM, the overall joint thermal contact resistance, $TCR_{J,TIM}$, for contacting surfaces can be given, as:

$$\boldsymbol{TCR_{J,TIM}(T_j, P) = TCR_{I,1} + TCR_{I,2} + \frac{t_o\left[1-P/E_{TIM}\right]}{k_{TIM}(T_j)}}, \quad \textbf{(2)}$$

where is P is the contact pressure, E_{TIM} is the Yung's modulus of the TIM, t_o is the initial TIM thickness, k_{TIM} is the TIM thermal conductivity, and TCR_I is the interface thermal contact conductance. As a first approximation, the average TIM temperature, T_j, can be defined as a simple average of interface temperatures on either side of TIM (Figure 1), as:

$$\boldsymbol{T_j = \left(T_{i,1,2} + T_{i,2,2}\right)/2}. \quad \textbf{(3)}$$

The energy transport across interfaces occurs also by thermal radiation, in parallel with the conduction. As it is customary to include an effective thermal contact conductance (TCC) for the thermal radiation, the equation for the overall TCR for interface "n," is cast in terms of the conduction component, $TCC_{C,I}$, and thermal radiation component, $TCC_{R,I}$ of the TCC, as:

$$\boldsymbol{TCR_{I,n} = \frac{1}{TCC_{C,I,n}+TCC_{R,I,n}}}. \quad \textbf{(4)}$$

For contacting surfaces, the "radiation" conductance was found to be negligible at joint temperatures below 700 K [4]. For this assessment in [4] a baseline conduction $TCC_{C,I}$ of 397 W/m^{2}K was used. When the contacting bodies are made of the same material, TCR_I was considered to be the same for both TIM-metal interfaces, i.e., $TCR_{I,1} = TCR_{I,2}$. However, when the contacting bodies are made of different materials, this assumption may not be applicable.

3 SURFACE ROUGHNESS CHARACTERIZATION AND INTERFACE TCC MODELS

The nature of contact depends on the surface roughness characteristics [4]. When the surface profile is locally Gaussian (i.e., its asperities are isotropic and randomly distributed), Ling [5] showed that the root mean square (RMS) roughness, σ, and the arithmetic average of the absolute values of the measured profile height deviations, *Ra*, are related through a relationship, as:

$$\boldsymbol{\sigma = \sqrt{\frac{\pi}{2}} R_a} \text{ (or } \boldsymbol{1.25 R_a}\text{)} \quad \textbf{(5)}$$

As reviewed in [4], Tanner and Fahoum [6], and Antonetti et al. [7] analyzed published experimental surface roughness data, and provided empirical correlations that relate the RMS asperity slope, m_q, to average roughness, *Ra*. Similar, Lambert and Fletcher [8], correlated the absolute average asperity slopes, *m*, as a function of RMS roughness in micrometers, as:

$$\boldsymbol{m = a_2 \sigma^{b_2}} \text{ (or } \boldsymbol{m = 0.085468\, {R_a}^{b_2}}\text{)}, \quad \textbf{(6)}$$

where a_2=0.076 and b_2=0.52 [8]. This dependence can be used to evaluate m when Ra is provided without the availability of the actual profilometry data. Closure models for the plastic and elastic thermal contact conduction interface TCC_I models for conforming rough surfaces are given in Table 1.

Table 1. Plastic and elastic thermal contact conduction interface TCC_I models for conforming rough surfaces.

Plastic contact conductance model	Elastic contact conductance model
$\boldsymbol{TCC_I(P) = a_1 k_s \frac{m}{\sigma}\left(\frac{P}{H_C}\right)^{b_1}}$ a_1=1.25, b_1=0.95 for soft on hard surfaces [9] a_1=1.45, b_1=0.985 for hard surfaces [10, 11]	$\boldsymbol{TCC_I(P) = a_1 k_s \frac{m}{\sigma}\left(\frac{P}{H_E}\right)^{b_1}}$ a_1=1.55, b_1=0.94 for soft on hard surfaces [9]
$\boldsymbol{H_C = P\left[\frac{P}{c_1(1.62\sigma[\mu m]/m)^{c_2}}\right]^{\frac{-1}{1+0.071c_2}}}$ [9, 12] The Vickers microhardness correlation coefficients c1 and c2, are related to the Brinell hardness by relationships given in [9, 13] for 1.3 ≤ HB ≤ 7.6 GPa. $\sigma[\mu m]$ is given in microns [4].	$\boldsymbol{H_E = \frac{m}{\sqrt{2}\left(\frac{1-\nu_i^2}{E_i} + \frac{1-\nu_m^2}{E_m}\right)}}$
$\boldsymbol{\mathrm{erfc}\left(\frac{\lambda}{\sqrt{2}}\right) = \frac{2P}{H_C}}$ [11, 14]	$\boldsymbol{\mathrm{erfc}\left(\frac{\lambda}{\sqrt{2}}\right) = \frac{4P}{H_E}}$ [14]

4 INTERFACE AND JOINT TCC IN VACUUM

The thermal contact resistance, TCR_J, or its reciprocal, thermal contact conduction, TCC_J, for the overall joint is usually estimated directly from temperature measurements, such as those using thermocouples. While most studies were conducted in air and/or in other gas environments [15], there are only few studies that were conducted in vacuum [16].

One of the main challenges in using TIM is the lack of data on interface TCC, as it cannot be accurately estimated from the TCR_J data or cannot be readily calculated using the correlation models shown in Table 1. This is mainly due to the fact few studies report all the data needed to estimate TCC. For example, data on roughness parameters m and σ are often not reported. Usually, TIM thickness are very small (sub mm), and the thickness evolution due to contact pressure variation is not reported. Thus, it is not uncommon to calculate "negative" numbers interface TCC_I, using the limited reference data. For example, using the data in [17] of TCC_J=1.3e+4 W/m^{2}K, nominal 0.35 mm Sigraflex FG, and nominal Sigraflex thermal conductivity of 5 W/mK, one obtains TCC_I=-0.14 W/m^{2}K.

Savija et al. [16] measured TCR_J as a function of contact pressure, i.e., $TCR_J(P)$, for the Al2024-grafoil-Al2024 system in both vacuum and air atmospheres at contact pressures of 0.2 MPa < P < 6.5 MPa. The data was presented at loading and unloading of grafoil sheets. Three nominal thicknesses were tested: 0.127mm (GTA 005), 0.381mm (GTA 015), and 0.762mm (GTA 030). Moreover, $TCR_J(P)$ was measured not only for one sheet of FG but also for stacks of two and three sheets. The data reported by Savija et al. [16] was obtained with the Bulk Resistance Method (BRM), which was developed in [9]. The BRM method can be used to estimate the joint thermal resistance, $TCR_J(P)$, interface $TCR_I(P)$ based on

analytical expressions, thermal conductivity (k_m), and Young's modulus (E_m) by taking into account the in-situ changes in material thickness due to external loading (Table 2). The linear variation of the TIM thickness with the contact pressure for FG was reported in [16]. In [16], the following mechanical properties were used to estimate TCC: (a) E_i=7.3e+10 MPa and Poisson's ratio 0.33 for Al2024 and (b) Poisson's ratio of 0.3 for grafoil.

Table 2. Surface characteristics of Grafoil GTA specimens, measured initial and final thickness and estimated thermal conductivity and Young's elastic modulus [16].

Specimen	No. of Sheets	t_0 $[mm]$	σ_m $[\mu m]$	m_m $[rad]$	Waviness $[\mu m]$	k_m $[W/mK]$	E_m $[MPa]$	t_f $[mm]$
1 GTA 005	1	0.14	1.35	0.055	19.35	4.36	19.11	0.13
2 GTA 005	2	0.27	1.44	0.070	10.75	5.29	30.44	0.25
3 GTA 005	3	0.42	1.41	0.062	12.18	5.10	44.06	0.37
1 GTA 015	1	0.40	1.84	0.072	11.60	7.62	28.37	0.34
2 GTA 015	2	0.78	1.89	0.070	16.73	6.81	35.85	0.67
3 GTA 015	3	1.17	1.81	0.070	12.53	7.31	36.82	0.98
1 GTA 030	1	0.80	1.66	0.062	11.70	5.95	40.95	0.69

1.1 TCC EVALUATION USING ELASTIC DEFORMATION MODELS FOR AL2024-GRAFOIL INTERFACES

The interface TCR_I was estimated in Tables 3, 4, and 5 at contact pressures of 0.2, 0.5, and 1 MPa, respectively, using the thermal conductivity (k_m) and Young's modulus (E_m) from Table 2 by calculating the FG thickness using Equation 1, as follows:

1. $TCR_J(P), P$ data was obtained by digitizing data from [16].
2. FG thickness was calculated for each contact pressure, as $\boldsymbol{t(P) = t_o\left[1 - P/E_{TIM}\right]}$ using the estimated E_{TIM} shown in Table 2 (original from [16]).
3. $\boldsymbol{TCR_I(P) = 0.5 * \left(TCR_J - \frac{t(P)}{k_{TIM}(T)}\right)}$ and $\boldsymbol{TCC_I(P) = \frac{1}{TCR_I(P)}}$.

Savija et al. [16] did not provide which formulation, i.e., elastic or plastic (as shown in Table 1), was used to evaluate $TCC_I(P)$. Hence, the elastic $TCC_{E,I}$ was first evaluated for all three contact pressures. As shown in Tables 3, 4, and 5, the elastic TCC is very high, as high as 10X than the estimated TCC_I. Thus, the plastic formulation was used to calculate the $TCC_I(P)$ in Savija et al. [16]. For the sake of completion, the plastic contact hardness of the grafoil, which is the softer material, was calculated, as:

$$\frac{H_C}{P} = \left(\frac{a_1 k_s\, m}{\sigma\, TCC_I(P)}\right)^{1/b_1}. \qquad \textbf{(7)}$$

To calculate ks, the thermal conductivity of Al2024 was considered to be 135 W/(mK) while for grafoil, the km data from Table 2 was used.

The calculated H_C ranges in values from 1 to 15 MPa, in good agreement with data reported in [3]. The calculated H_C can then be used to estimate TCC_I based on the plastic formulations for other interfaces, such as grafoil-tungsten and grafoil-glidcop, which are considered in the MPEX project.

Table 3. Estimated interface TCC_I(0.2 MPa) and TCR_I(0.2 MPa) in vacuum for Grafoil GTA at P_1=0.2 MPa contact pressure using measured and estimated data from Savija et al. [16].

Specimen	No. of Sheets	t_I [mm]	$TCR_J(P_1)$ [m²K/W]	$TCR_I(P_1)$ [m²K/W]	$TCC_I(P_1)$ [W/m²K]	$TCC_{E,I}(P_1)$ [W/m²K]	$H_C(P_1)$ [MPa]
1 GTA 005	1	0.139	1.835e-04	7.586e-05	13.18e+03	161.57e+03	6.8713
2 GTA 005	2	0.268	1.638e-04	5.655e-05	17.68e+03	99.226e+03	7.3665
3 GTA 005	3	0.415	-	-	-	71.075e+03	-
1 GTA 015	1	0.398	2.199e-04	8.388e-05	11.921e+03	83.108e+03	12.461
2 GTA 015	2	0.776	3.433e-04	1.147e-04	8.719e+03	64.830e+03	14.494
3 GTA 015	3	1.164	3.718e-04	1.063e-04	9.406e+03	66.018e+03	15.006
1 GTA 030	1	0.796	3.608e-04	1.135e-04	8.808e+03	64.669e+03	12.719

Table 4. Estimated interface TCCI(0.5 MPa) and TCRI(0.5 MPa) in vacuum for Grafoil GTA at P_2=0.5 MPa contact pressure using measured and estimated data from Savija et al. [16].

Specimen	No. of Sheets	t_I [mm]	$TCR_J(P_2)$ [m²K/W]	$TCR_I(P_2)$ [m²K/W]	$TCC_I(P_2)$ [W/m²K]	$TCC_{E,I}(P_2)$ [W/m²K]	$H_C(P_2)$ [MPa]
1 GTA 005	1	0.136	5.968e-05	1.421e-05	70.36e+03	3.8232e+05	3.2179
2 GTA 005	2	0.266	6.667e-05	8.239e-06	121.4e+03	2.3480e+05	2.6820
3 GTA 005	3	0.415	1.549e-04	3.674e-05	27.22e+03	1.6818e+05	10.446
1 GTA 015	1	0.393	1.092e-04	2.878e-05	34.75e+03	1.9666e+05	10.687
2 GTA 015	2	0.769	1.693e-04	2.816e-05	35.51e+03	1.5340e+05	8.8970
3 GTA 015	3	1.15	2.041e-04	2.309e-05	43.30e+03	1.5622e+05	8.1496
1 GTA 030	1	0.790	2.456e-04	5.638e-05	17.74e+03	1.5302e+05	15.787

Table 5. Estimated interface TCCI(1 MPa) and TCRI(1 MPa) in vacuum for Grafoil GTA at P_3=1 MPa contact pressure using measured and estimated data from Savija et al.

Specimen	No. of Sheets	t_I [mm]	$TCR_J(P_3)$ [m²K/W]	$TCR_I(P_3)$ [m²K/W]	$TCC_I(P_3)$ [W/m²K]	$TCC_{E,I}(P_3)$ [W/m²K]	$H_C(P_3)$ [MPa]
1 GTA 005	1	0.133	3.556e-05	2.575e-06	388.4e+03	7.3349e+05	1.1659
2 GTA 005	2	0.261	5.905e-05	4.838e-06	206.7e+03	4.5046e+05	3.1505
3 GTA 005	3	0.411	9.143e-05	5.449e-06	183.5e+03	3.2266e+05	3.0990
1 GTA 015	1	0.386	5.538e-05	2.348e-06	426.0e+03	3.7729e+05	1.7435
2 GTA 015	2	0.758	1.218e-04	5.242e-06	190.8e+03	2.9431e+05	3.3117
3 GTA 015	3	1.14	1.693e-04	6.834e-06	146.3e+03	2.9971e+05	4.8240
1 GTA 030	1	0.780	1.484e-04	8.604e-06	116.2e+03	2.9358e+05	4.8204

5 TCC EVALUATION FOR TUNGSTEN-GRAFOIL AND GLIDCOPAL15-GRAFOIL INTERFACES

As shown in the previous section, the plastic formulation has to be used to evaluate the $TCC_I(P)$ for other metal-grafoil interfaces, such as tungsten-grafoil and GlidcopAl15-grafoil interfaces are often considered in the plasma-interface materials (PMI) testing facilities, such as the MPEX facility at ORNL. Thus, the plastic contact conductance at interface "n" is given by:

$$\boldsymbol{TCC_{P,I,n}(P,T) = a_1 k_s(T) \frac{m_{eff,n}}{\sigma_{eff,n}} \left(\frac{P}{H_C(P)}\right)^{b_1}}, \quad \textbf{(8)}$$

where a_1=1.25, b_1=0.95 for soft on hard surfaces [9].

In order to estimate k_s, data on thermal conductivity of materials considered is provided. The temperature dependence of thermal conductivity for grafoil, W, and Glidcop-Al15 were obtained from [1, 2], [18], and [19], respectively, and are shown in Figure 2a. First, the k_s was estimated for the grafoil-Al2024, grafoil-W, and grafoil-glidcop interfaces. In the absence of reported data for Glidcop-Al15 above 873K, its thermal conductivity was considered to be constant at values larger than 873K (and less than its melting point of 1356K). Analytical expressions for the thermal conductivity variation with temperature of W, grafoil, and glidcop-Al15 are shown in Appendix A. Since thermal conductivity in the normal direction to the grafoil sheet is very small (approx. 5 W/mK), and the thermal conductivity of Al2024, W, and glidcop-Al15 is much higher than that of the grafoil, k_s was found to exhibit similar values for all three interfaces considered (Figure 2b). For example, at room temperature, k_s was estimated to be approx. 9.6 W/mK for all three interfaces considered (W-grafoil, Glid-grafoil, Al2024- grafoil).

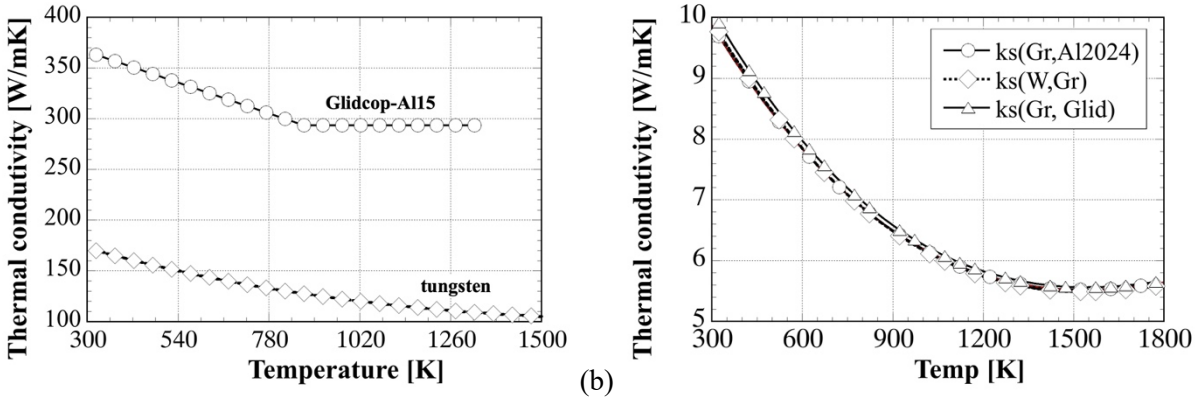

Figure 2. (a) Thermal conductivity of materials considered and (b) estimated ks estimate for material pairs considered.

The effective m and σ can be estimated, as:

$$\boldsymbol{\sigma_{eff,n} = \sqrt{\sigma_n{}^2 + \sigma_m{}^2}} \text{ and } \boldsymbol{m_{eff,n} = \sqrt{m_n{}^2 + m_m{}^2}}, \quad \textbf{(9)}$$

using σ_n, σ_m, m_n, and m_m which have to be obtained directly from profimetry measurements, where *n* indicates the interface (e.g., 1 for tungsten-grafoil and 2 for GlidcopAl15-grafoil). Alternatively, *m* and σ at each interface can be obtained using Eq. 6 as a function of individual *Ra*.

As a first step to evaluating the TCC_I using Eq. 8, it is considered that the effective roughness parameters m and σ are those from [9]. In this case, the same TCC_I would be predicted for the W-grafoil and Glidcop-grafoil interfaces. Moreover, the temperature variation of the TCC_I maybe considered through the k_s variation. However, other factors, such as $H_C(P)$ temperature variation and contact pressure within the system need to be considered. Still, due to its high-temperature rating (up to 3270K in vacuum/reducing environments) it could be likely that $H_C(P)$ may exhibit a weak temperature variation for the temperature range envisioned for PMI operation of this joint (e.g., 1270-1770°C).

6 RADIATION THERMAL CONTACT CONDUCTANCES IN VACUUM

The energy transport across interfaces occurs also by thermal radiation, even when the surfaces are not separated. The TCC, which describes the energy transport across interfacial gaps at contacting interfaces, is given by [20]:

$$\boldsymbol{TCC_{R,I}(T_{I,1}, T_{I,2}) = \sigma_{SB}\epsilon_{12}\frac{T_{I,1}^4 - T_{I,2}^4}{T_{I,1} - T_{I,2}}}, \quad \textbf{(10)}$$

where σ_{SB}=5.67037442e-8 W/m^{2}K^4 is the Stefan Boltzman constant. The effective emissivity between two parallel plates that are considered to be gray bodies, $\boldsymbol{\epsilon_{12}}$, is given, as a function of surface emissivities, as [20]:

$$\boldsymbol{\frac{1}{\epsilon_{12}} = \frac{1}{\epsilon_n} + \frac{1}{\epsilon_m} - 1}, \quad \textbf{(11)}$$

where n indicates the interface (e.g., 1 for tungsten-grafoil and 2 for GlidcopAl15-grafoil). The emissivity of grafoil and tungsten were ϵ_m=0.5 [1] and ϵ_1=0.1-0.18 (1000-1500K) [21], respectively. Thus, $\boldsymbol{\epsilon_{12}}$ for tungsten-grafoil can vary from 0.09 to 0.15 for temperatures between 1000-1500K.

Data on emissivity for GlidcopAl15 is not available in the literature and data for Cu can be used as GlidcopAl15 (contains 0.3 wt. % Al_2O_3 and Cu balance). Cu emissivity depends on its condition (i.e., oxidized or not). The following emissivity, ϵ_2, were found in the Cindas database: 0.018 (603-1110K), 0.05 (538-923K), 0.03 (1111K), and 0.34-0.82 (624-1063K) for polished, shot-blasted (stabilized at 900K), mechanically polished (heated at 450 K in air for 3 hours and at 922 K in air for 3 hours and then kept at 1242 K in vacuum for 45 hours), and extreme oxidation (stably oxidized at 1033K). Since for our application the oxidation is not desired (oxide layer would lower the interface TCC), the surface of the glidcop is considered to be not heavily oxidized. Based on the above review data, ϵ_2=0.05, which is the highest among all conditions indicated (excluding the heavy oxidized condition). Thus, ϵ_{12} for GlidcopAl15-grafoil is likely to be approximately 0.048.

When the temperature variation across interface is small, Equation 10 can be cast as a function of the average joint temperature, which is given by Equation 2, as:

$$\boldsymbol{TCC_{R,I}(T_I) = 4\sigma_{SB}\epsilon_{12}T_I^3} \quad \textbf{(12)}$$

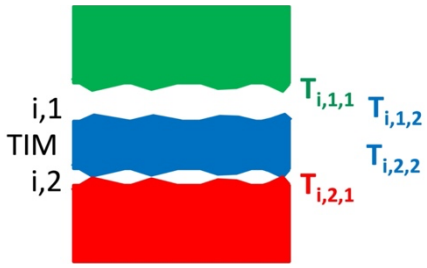

Figure 3. Possible separation of TIM from hard materials during high-heat flux operation.

Referring to Figure 3, and considering effective emissivities for the interfaces considered according to Equation 11, following the "radiation" thermal contact conductances can be obtained:

$$\boldsymbol{TCC_{R,1}(T_{i,1,1}, T_{i,1,2}) = 0.045\,\sigma_{SB}\left(T_{i,1,1} + T_{i,1,2}\right)^3} \text{ for W-grafoil interface} \quad \textbf{(13)}$$

$$\boldsymbol{TCC_{R,2}(T_{i,2,1}, T_{i,2,2}) = 0.024\,\sigma_{SB}\left(T_{i,2,1} + T_{i,2,2}\right)^3} \text{ for GlidcopAl15-grafoil interface} \quad \textbf{(14)}$$

The steady state temperature differences across interfaces, i.e., $T_{i,1,1} - T_{i,1,2}$ and $T_{i,2,1} - T_{i,2,2}$, can be obtained through an iterative approach, assuming that the average heat flux and back side temperature of the glidcop are known.

1. Start new iterations with previous $T_{i,1,1}, T_{i,1,2}$, $T_{i,2,1}$, and $T_{i,2,2}$
2. Evaluate $TCC_{R,1}(T_{i,1,1}, T_{i,1,2})$, $TCC_{R,2}(T_{i,2,2}, T_{i,2,1})$
3. Update Tmax on top surface accounting for all thermal contact conductances through the Glidcop, GlidcopAl15-grafoil, grafoil, and W-grafoil
4. Update $T_{i,1,1}$ based on Tmax and q"average
5. Update $T_{i,1,2}$, from $T_{i,1,1} - T_{i,1,2} = \frac{q"_{ave}}{TCC_{R,1}(T_{i,1,1}, T_{i,1,2})}$
6. Update $T_{i,2,2}$, from $T_{i,1,2} - T_{i,2,2} = t_o \frac{q"_{ave}}{k_{TIM}(T_j)}$
7. Update $T_{i,2,1}$, from $T_{i,2,2} - T_{i,2,1} = \frac{q"_{ave}}{TCC_{R,2}(T_{i,2,2}, T_{i,2,1})}$
8. Check convergence of $T_{i,2,1}$ by comparing with previous value; if convergence attained, stop, otherwise start a new iteration

Without employing the more accurate iterative approach, the $TCC_{R,1}(T_{i,1,1}, T_{i,1,2})$ is shown in Figure 4 as a function of the average temperature across this interface $(T_{i,1,1}, T_{i,1,2})$. This data is shown for the sake of completion. It shows that that $TCC_{R,1}(T_{i,1,1}, T_{i,1,2})$ would be at best 0.01X than its conductance $TCC_I(P_1)$, which is shown in Table 3.

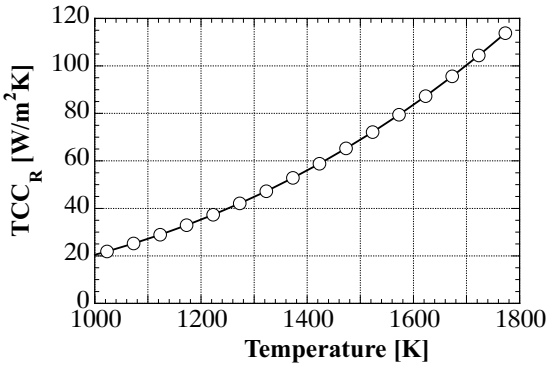

Figure 4. Radiation TCC for W-grafoil interface as a function of average temperature across the interface.

7 RECOMMENDATIONS FOR TCC IN VACUUM: W-GRAFOIL AND GLIDCOPA15-GRAFOIL INTERFACES

In the absence of surface roughness data (Section 3.2), the following TCC_I can be recommended on either side of grafoil (W, or Glidcop-Al15) based on the data presented in Sections 3.1 and 3.3, and the analysis conducted in Section 3.2:

1. $TCC_I(P) = TCC_{R,1}$ for contact pressures P<0.01 P_1
2. $TCC_I(P) = \left(\frac{P}{P_1} - 0.01\right) TCC_I(P_1) + TCC_{R,1}$ for contact pressures $0.01\ P_1 < P < P_1$
3. $TCC_I(P_1)$=1.0e+4 W/m^{2}K for contact pressure of P_1=0.2 MPa
4. $TCC_I(P_2)$=3.0e+4 W/m^{2}K for contact pressure of P_2=0.5 MPa
5. $TCC_I(P_3)$=1.5e+5 W/m^{2}K for contact pressure of P_3=1 MPa

8 REFERENCES

1. Pollock, M., *GRAFOIL® Flexible Graphite, Engineering Design Manual.* Copyright, 2002.
2. Solfiti, E. and F. Berto, *A review on thermophysical properties of flexible graphite.* Procedia Structural Integrity, 2020. **26**: p. 187-198.
3. Khelifa, M., et al., *Nanoindentation of flexible graphite: yxperimental versus simulation studies.* Advanced materials science, 2018. **3**(2): p. 1-11.
4. Bahrami, M., *Modeling of thermal joint resistance for sphere-flat contacts in a vacuum.* 2004.
5. Ling, F., *On asperity distributions of metallic surfaces.* Journal of Applied Physics, 1958. **29**(8): p. 1168-1174.
6. Tanner, L. and M. Fahoum, *A study of the surface parameters of ground and lapped metal surfaces, using specular and diffuse reflection of laser light.* Wear, 1976. **36**(3): p. 299-316.
7. Antonetti, V., T. Whittle, and R. Simons, *An approximate thermal contact conductance correlation.* 1993.
8. Lambert, M.A. and L.S. Fletcher, *Thermal Contact Conductance of Spherical Rough Metals.* Journal of Heat Transfer, 1997. **119**(4): p. 684-690.
9. Savija, I., J. Culham, and M. Yovanovich. *Effective thermophysical properties of thermal interface materials: part I—definitions and models*. in *International Electronic Packaging Technical Conference and Exhibition*. 2003.

10. Yovanovich, M.M., *Four decades of research on thermal contact, gap, and joint resistance in microelectronics.* IEEE transactions on components and packaging technologies, 2005. **28**(2): p. 182-206.
11. Cooper, M., B. Mikic, and M. Yovanovich, *Thermal contact conductance.* International Journal of heat and mass transfer, 1969. **12**(3): p. 279-300.
12. Song, S. and M. Yovanovich, *Relative contact pressure-Dependence on surface roughness and Vickers microhardness.* Journal of thermophysics and heat transfer, 1988. **2**(1): p. 43-47.
13. Sridhar, M. and M. Yovanovich, *Empirical methods to predict Vickers microhardness.* Wear, 1996. **193**(1): p. 91-98.
14. Yovanovich, M., *New contact and gap conductance correlations for conforming rough surfaces.* AIAA Paper, 1981(81-1164): p. 1-6.
15. Marotta, E.E., S.J. Mazzuca, and J. Norley, *Thermal joint conductance for flexible graphite materials: analytical and experimental study.* IEEE Transactions on Components and Packaging Technologies, 2005. **28**(1): p. 102-110.
16. Savija, I., J. Culham, and M. Yovanovich. *Effective thermophysical properties of thermal interface materials: part II—experiments and data*. in *International Electronic Packaging Technical Conference and Exhibition*. 2003.
17. Greuner, H., et al., *Final design of W7-X divertor plasma facing components—tests and thermo-mechanical analysis of baffle prototypes.* Fusion engineering and design, 2003. **66**: p. 447-452.
18. N.B., V., *Thermophysical properties of substances*. 1956, Moscow-Leningrad: Gosénergoizdat.
19. Jin, J., W. Xiao, and H. Chen. *Thermal Fatigue Life of Glidcop Al-15 High-Heat-Load Components*. in *AIP Conference Proceedings*. 2010. American Institute of Physics.
20. Howell, J.R., et al., *Thermal radiation heat transfer*. 2020: CRC press.
21. Matsumoto, T., A. Cezairliyan, and D. Basak, *Hemispherical total emissivity of niobium, molybdenum, and tungsten at high temperatures using a combined transient and brief steady-state technique.* International Journal of thermophysics, 1999. **20**(3): p. 943-952.

APPENDIX A. MATERIALS PROPERTIES

Thermal conductivity dependence is given in a format implemented in the CFX software.

```
kGlidcopAL15 = 369.43[W m^-1 K^-1]-0.126708[W m^-1 K^-2]*(T-273.15[K])
    kTungsten = 174.9274[W m^-1 K^-1] - 0.1067[W m^-1 K^-2]*(T-273.15[K])+ \
      5.0067E-5[W m^-1 K^-3]*(T-273.15[K])^2- 7.8349E-9[W m^-1 \
      K^-4]*(T-273.15[K])^3
    kgrafoilNormalDir = 5.24339[W m^-1 K^-1]-4.49081e-03[W m^-1 \
      K^-2]*(T-273.15[K])+2.54786e-06[W m^-1 \
      K^-3]*(T-273.15[K])^2-4.05899e-10[W m^-1 K^-4]*(T-273.15[K])^3
```